MICROMECHANICAL CHARACTERIZATION OF DAMAGE IN CEMENT PASTES: AN EXPERIMENTAL-NUMERICAL STUDY

ABDERRAHMANE RHARDANE, FREDERIC GRONDIN AND SYED YASIR ALAM

Institut de Recherche en Génie Civil et Mécanique, GeM-UMR 6183, Centrale Nantes –
Université de Nantes – CNRS, 1 rue de la Noë, 44321 Nantes, FRANCE
e-mail: {abderrahmane.rhardane; frederic.grondin; syed-yasir.alam}@ec-nantes.fr, www.ec-nantes.fr

Key words: Damage, Cement paste, Cement phases, Micromechanics, Macroscopic properties

Abstract: A modelling approach is proposed for the simulation of damage in cement pastes at the microscale. The approach takes use of recent advances in hydration modelling tools and the experimental and numerical characterization of micromechanical properties of cement paste phases. It is shown that the modelling approach can illustrate the damage behaviour of the cement matric and predict the properties of well-hydrated cement pastes. It can therefore be used to calculate the macroscopic properties of cement pastes as well as investigate the propagation of damage inside the cement paste matrix without the need for a new identification of model parameters. Some of the limitations to the presented approach are also discussed.

1 INTRODUCTION

Cracking in concrete is essentially driven by damage in the binding cement matrix (bulk cement paste and ITZ). Therefore, the study of damage at smaller scales is a prerequisite for the understanding of the mechanical behaviour of cementitious materials under mechanical loads as well as in response to various environmental solicitations, such as thermal cracking, freeze-thaw, creep and shrinkage, since the underlying mechanisms emerge at the microscale.

The characterization of the mechanical behaviour of cement pastes, and particularly of damage at the microscopic scale, has been a long-standing challenge due to the complex microstructure of the hardening cement paste. In fact, a thorough description requires the knowledge of the intrinsic properties of cement phases as well as their interactions within the heterogeneous microstructure. Thanks to advances in experimental and numerical techniques such as nanoindentation [1]–[4] and molecular dynamics [5], cement paste phases have been identified and their properties determined. Consequently, many studies have used these findings to calculate the macroscopic elastic properties of cement pastes using virtual microstructures generated by hydration models [6]–[9]. The success of such a micromechanical approach has led authors to simulate the cracking behaviour of cement pastes [10]–[13]. Nevertheless, some challenges still persist, such as the lack of micromechanical properties pertinent to the fracture of cement phases and the absence of experimental validation for different cement paste compositions.

In this study, the virtual microstructure of cement paste is created using the VCCTL hydration modelling platform, based on the kinetics code of CEMHYD3D [14]. The microstructure is then introduced in the finite element code Cast3M 2016 [15]. Unlike other studies where a perfectly brittle damage model is used, an adequate damage model accounting for a softening behaviour is chosen instead. A review of the intrinsic properties of cement paste phases presented in the literature is

conducted, demonstrating the lack of certain properties pertinent to damage modelling such as strength and fracture energy. The effective values of these properties are determined using inverse analysis, based on experimental data obtained at the macroscale from a reference cement paste. The micromechanical approach is then laid down and applied to calculate the mechanical properties of cement pastes with various cements and different w/c ratios. It is shown that the proposed micromechanical approach is able to predict the properties of cement pastes such as Young's modulus, tensile and compressive strength as well as fracture energy in a satisfactory manner. The limitations of this approach are discussed and the potential of the micromechanical approach to simulate multi-physical problems at the microscale is also explored.

2 MICROMECHANICAL MODELLING OF DAMAGE IN CEMENT PASTE

The proposed micromechanical approach follows the line of reasoning introduced in previous studies (see [8], [10], [11]). First, a virtual microstructure of cement paste is generated using the VCCTL platform. The representative elementary volume (REV) created using the hydration model takes into account the size distribution and the assemblage of cement phases in the paste. The REV is then converted into a finite element mesh using the code Cast3M. A damage model is applied for all cement phases, allowing for damage resistance due to the inherent strength and fracture energy of each phase. The fracture parameters of cement phases are considered intrinsic and therefore independent of the cement paste composition. The macroscopic properties of the paste thus depend on the volume fractions of the phases as well as their arrangement.

2.1 Microstructure generation

The first step of the modelling approach is the construction of a virtual microstructure of cement paste. Among the many hydration models proposed in the literature (see [4] for some examples), the VCCTL platform [16] is

chosen. The voxelized architecture and the explicit representation of cement phases make it simple to integrate the REV in finite element codes. The code requires classical information about cement mixtures such as the mineral composition of the unhydrated phases (clinker, gypsum, additives, etc.), the particle size distribution, and input data pertaining to mix design conditions, such as the water-to-cement ratio, the activation energy of hydration reactions, the temperature and the curing conditions. The code constructs an initially-saturated mix composition, and then mimics the dissolution-precipitation steps of phase reactions, using a kinetic cellular automaton. It should be noted that the model can be used without any need for parametric setting, and can therefore be used for a variety of cement compositions. The final output of the code is a microstructure of cement paste, evolving with age. Throughout the proposed study, many microstructures are generated and for different purposes. These are described in sections 3 and 4. Figure 1 illustrates an evolving microstructure of cement paste constructed via VCCTL and meshed using Cast3M.
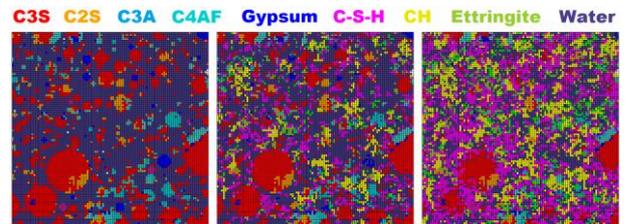
Figure 1: Evolving microstructure of cement paste constructed by VCCTL (colour code represents the primary cement phases).

2.2 Damage model

Cement phases are explicitly represented in the REV generated by the hydration model. This allows for an attribution of different behaviours to distinct phases. For the sake of simplicity, the same damage model is applied with different parameters. The damage model developed by Fichant et al. [17], [18] and widely used for the damage characterization of cementitious materials is used. In the isotropic version of the model, the stress-strain relationship reads:

$$\boldsymbol{\sigma} = \left(1 - D_T\right)\left\{\mathbb{C}^0\boldsymbol{\varepsilon}\right\}_+ + \left(1 - D_C\right)\left\{\mathbb{C}^0\boldsymbol{\varepsilon}\right\}_- \qquad (1)$$

Where D_T and D_C are respectively the damage variables in tension and in compression. $\mathbb{C}^0$ is the stiffness tensor of the undamaged state and the Macaulay brackets $\{\bullet\}$ separate the tensile and compressive components of the effective stress tensor. In the absence of plasticity, the loading surface is written in terms of the Mazars equivalent strain ε_{eq} and the damage threshold κ_0:

$$f = \varepsilon_{eq} - \kappa_0 \qquad (2)$$

With the equivalent strain calculated using the principal tensile strains of the strain tensor:

$$\varepsilon_{eq} = \sqrt{\sum \left\{\varepsilon_{ii}\right\}_+^2} \qquad (3)$$

To incorporate the tension-compression dissymmetry, the damage evolution law in tension takes the exponential form:

$$D_T = 1 - \frac{\kappa_0}{\varepsilon_{eq}}\exp\left[-B_T\left(\varepsilon_{eq} - \kappa_0\right)\right] \qquad (4)$$

Where B_T is a parameter that controls the softening curve of the constitutive equation. The damage variable in compression D_C is linked to D_T via a coupling coefficient β:

$$D_C = D_T{}^{\beta} \qquad (5)$$

It is assumed that cement phases are broken only in opening mode I. Therefore, β is set to a high value in order to eliminate failure due to compression.

2.3 Micromechanical properties of cement phases

The Fichant model parameters attributed to each phase are linked to its micromechanical properties. The damage threshold depends on the tensile strength and the Young's modulus:

$$\kappa_0 = \frac{f_t}{E} \qquad (6)$$

Using energetic regularization [19], the softening parameter B_T depends on the fracture energy, such as:

$$B_T = \frac{f_t}{\dfrac{G_f}{h} - \dfrac{f_t^2}{2E}} \qquad (7)$$

Where h is the characteristic length that depends on the finite element size.

It can be seen that the damage model parameters depend entirely on the intrinsic properties of the cement phases, namely the elastic moduli E and v, the tensile strength f_t and the fracture energy G_f. The determination of these micromechanical properties has been the focus of many studies, particularly the elastic moduli (see [4], [6], [9], for example). As for f_t and G_f, very few studies [3], [20] give a quantitative estimation, and the data is lacking for the majority of cement phases. This poses a problem for mechanical modelling of damage at the lower scale. In order to determine the remaining properties, a new way of solving the issue is presented hereafter. Section 3 deals with the identification of the remaining fracture properties while section 4 presents a validation of the damage modelling approach against experimental results.

3 DETERMINATION OF THE INTRINSIC PROPERTIES OF CEMENT PHASES

3.1 Proposed calibration method

It is practically difficult, if not impossible, to identify the unknown properties of all the phases in a hydrated cement paste (the number varies between a dozen for Portland cement and more than fifty for composite cements). For this reason, certain assumptions are made:
- Each voxel (elementary volume of $1\mu m^3$) in the microstructure represents a single phase with a homogenised isotropic behaviour.
- All phases follow the same damage law.
- The tensile strength f_t of each phase is strongly dependent on its microindentation hardness HD, such as:

$$HD = \alpha f_t \qquad (8)$$

- The size-independent fracture energy G_f of the phase is linked to the strain energy [21]:

$$G_f = \beta(1+\nu)\frac{f_t^2}{E} \qquad (9)$$

The first assumption implies that the C-S-H gel is considered as a single phase composed of a mixture of low and high density C-S-H. The third and the fourth assumptions reduce the number of unknown parameters to α and β. At this stage, only the elastic moduli E and ν and the hardness HD are known for all phases, which are compiled from various sources (see Table 1 for a list of the main phase properties and [22] for a complete list). Knowing α and β, all the model parameters can be calculated.

A detailed parametric investigation was conducted, showing that each of these two parameters influences both the macroscopic strength and fracture energy of cement pastes in a nonlinear manner (cf. Figure 5). The parametric study also shows that for any given properties $f_{t,paste}$ and $G_{f,paste}$, there exists a unique pair (α, β) that corresponds to such macroscopic properties. This means that if the properties of a reference cement paste are known, they can be used to determine the unknown coefficients.
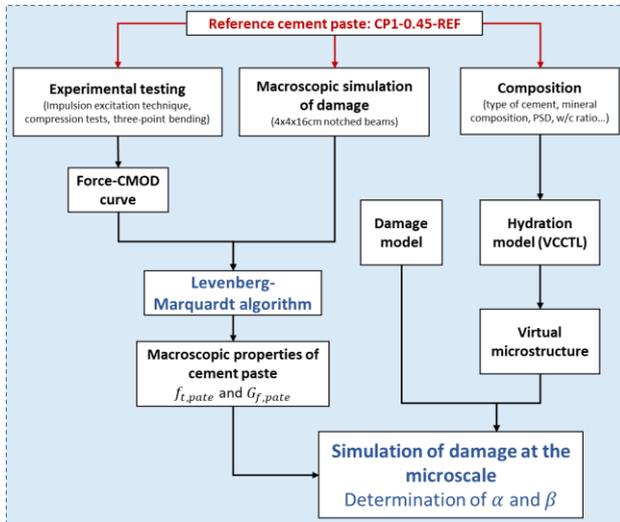
**Figure 2**: Inverse analysis scheme to determine the coefficients α and β.

Using these results, an inverse analysis scheme is laid down for the determination of α and β, as shown in Figure 2. First, multiple notched beams of size 4x4x16cm made from a reference cement paste labelled CP1-0.45-REF

(Portland cement type I, w/c =0.45, at 28 days) are tested under CMOD-controlled three-point bending in order to determine the global force-CMOD response of cement paste. On the other hand, the tested beams are simulated at the macro-level using Fichant's damage law, as shown in Figure 3. The main goal is to determine the macroscopic properties $f_{t,paste}$ and $G_{f,paste}$ that correspond to the global force-CMOD curve obtained earlier (see [19] for an application of this method to concrete). At this point, damage can be simulated at the microscale. The input data needed for the microstructure general are inserted, including the composition of the mix design. The microstructure is converted into a FE mesh and then the damage model is applied with the corresponding phase properties, using the equations 8 and 9.
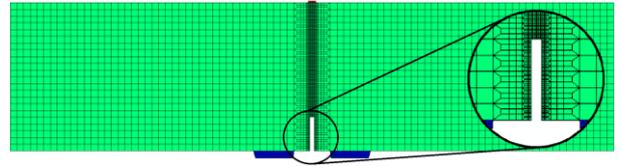
Figure 3: Macroscopic notched beam of cement paste subjected to three-point bending loading.

3.2 Experimental testing and simulation of damage at the macroscale
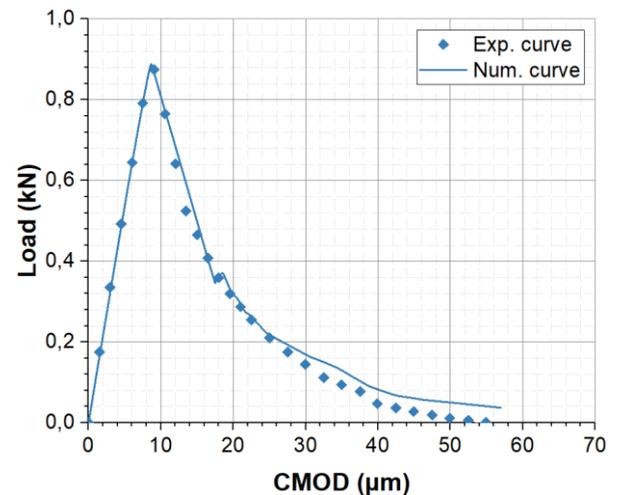
Figure 4: Experimental v. numerical F-CMOD curves.

Simulation of damage at the macroscale requires the knowledge of four macroscopic properties of cement paste (E_{paste}, ν_{paste}, $f_{t,paste}$
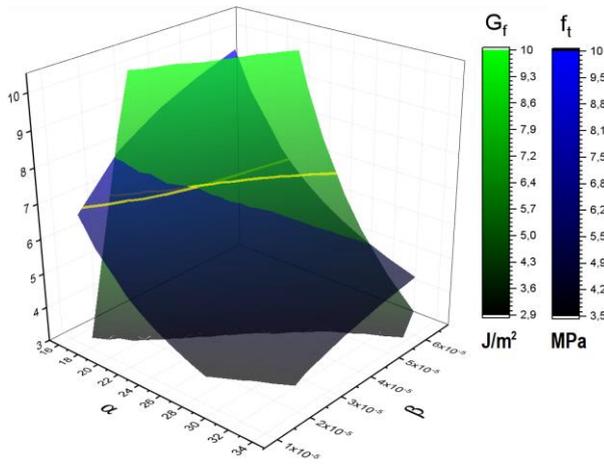
and $G_{f,paste}$). For this reason, three unnotched beams are first tested using the impulsion excitation technique in order to find the elastic moduli of CP1-0.45-REF. As for the unknown properties, the Levenberg-Marquardt algorithm was used. The idea is to find $f_{t,paste}$ and $G_{f,paste}$ which gives the numerical force-CMOD curve that is the most fitting to the experimental curve, as shown in Figure 4.

The properties found for CP1-0.45-REF are $f_{t,paste} = 6.77$MPa and $G_{f,paste} = 6.7$J/m².

3.3 Simulation of damage at the microscale

Knowing the macroscopic properties of the reference cement paste, the pair (α, β) can be determined. Figure 5 illustrates the evolution of the tensile strength and the fracture energy as a function of α and β. The isopleths of the surface curves with the constant planes formed by $f_{t,paste}$ and $G_{f,paste}$, shown in yellow, intersect at the point with the coordinates $\alpha = 20.2$ and $\beta = 3.75 \times 10^{-5}$. Once these two parameters are identified, the tensile strength and the fracture energy of all cement phases can be calculated from the already known properties (Table 1).

The effective properties identified using inverse analysis might not correspond to the actual physical properties of cement phases. However, they are useful to simulate damage of cement pastes through a calibration-free approach. The micromechanical properties of cement phases are considered as intrinsic values for all future cement compositions.

Table 1: Properties of the main cement paste phases.

Phase	E (GPa)	v (-)	f_t (MPa)	G_f (J/m²)
C_3S	137.4	0.30	430.7	65.8
C_2S	135.5	0.30	396.0	56.3
C_3A	145.2	0.28	534.6	94.3
C_4AF	150.8	0.32	470.3	72.5
Gypsum	44.5	0.33	29.6	0.98
CH	43.5	0.29	73.8	6.1
C-S-H	23.8	0.24	55.0	5.9
Ettringite	24.1	0.32	39.6	3.2
AFm	43.2	0.29	262.4	77.3

During the pre-peak region and before reaching 60% of the tensile strength (4.1MPa), no apparent microcracks form inside the paste. As the stress reaches the peak, microcracks appear randomly in the weakest zones (small C-S-H bridges, connected pores, etc.). As the stress decreases along the post-peak softening curve, microcracks start coalescing into bigger cracks, primarily through the poorly crystalline C-S-H gel and occasionally through other hydrates. The presence of unhydrated particles leads to crack arrest, branching and offset of 5-12µm due to the presence of CH crystals. Close to the complete failure of the cement paste, the crack profile shows an important coalescence of macrocracks throughout the cement paste, perpendicular to the direction of the loading (Figure 6).
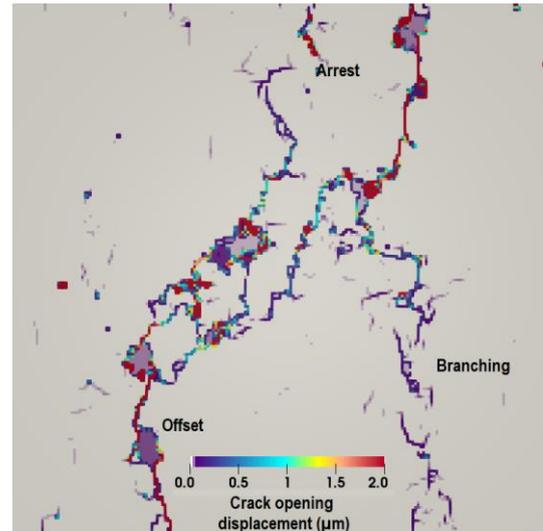
Figure 6: Crack opening displacement at 20% of maximum load in the post-peak region (cement paste is loading along the horizontal direction).

Figure 5: Evolution of the macroscopic tensile strength (blue) and fracture energy (green) as a function of the two parameters α and β.

5

4 VALIDATION OF THE MICROMECHANICAL APPROACH

The modelling approach has been used to determine the micromechanical properties of cement phases and has shown the ability to illustrate the damage behaviour at the micro-level. In this section, the same principles of the approach are applied for different cement compositions and under different loadings.

4.1 Validation method

In this validation step, the micromechanical approach is applied for five mix designs with different w/c ratios (0.4, 0.45 and 0.5) and at distinct ages (28 and 14 days) under tensile loading. These are labelled CP1-0.4-28d, CP1-0.4-14d, CP1-0.45-14d, CP1-0.5-28d and CP1-0.5-14d. A sixth mix design with cement type II is simulated under tension (CP2-0.45-28d). A second series of simulations is conducted for cement pastes under compressive loading. This is the case for the cement pastes CP1-0.4-28d, CP1-0.45-28d and CP1-0.5-28d. To complete this series, another set of examples under compression, derived from the literature, is also considered. Input data about cement composition for the hydration is taken from Nanocem database (see [23]). Cement pastes used in these simulations are not tested and the experimental data used for validation can be found in [24].

The same principles are applied for each example. The data concerning the mix design are injected into the hydration model in order to construct the corresponding microstructure. The microstructure is converted into the FE code and the phase properties identified in section 3 are applied. The macroscopic stress-strain curve of each example is calculated by volume averaging and the macro-properties are determined.

In this validation step, experimental testing is not needed since all the model parameters have been adjusted. Instead, experimental testing will be used for the sole purpose of comparison. For the tension simulations, the corresponding mix designs are experimentally studied using the three-point bending test for at least two 4x4x16cm notched beams. The F-CMOD curves are used in damage simulation at the macroscale (see Figure 3) to determine the properties of cement pastes (elastic moduli, tensile strength and fracture energy). For the compression simulations, 4x4x4cm cubes of cement paste are loaded under uniaxial compression to determine the compressive strength.

4.2 Results and discussion

In the case of tension, Table 2 and Table 3 show the macroscopic properties of cement pastes calculated using the micromechanical approach and from experimental results by inverse analysis, respectively. It can be seen that the micromechanical approach was able to approximate the experimental values for the elastic modulus ($\pm$0.7GPa), the tensile strength ($\pm$0.6MPa) and the fracture energy ($\pm$1.7J/m²) of different cement pastes to a satisfactory degree. The differences could be attributed to the variability of experimental measurements as well as the strong assumptions taken for the identification of the model parameters.
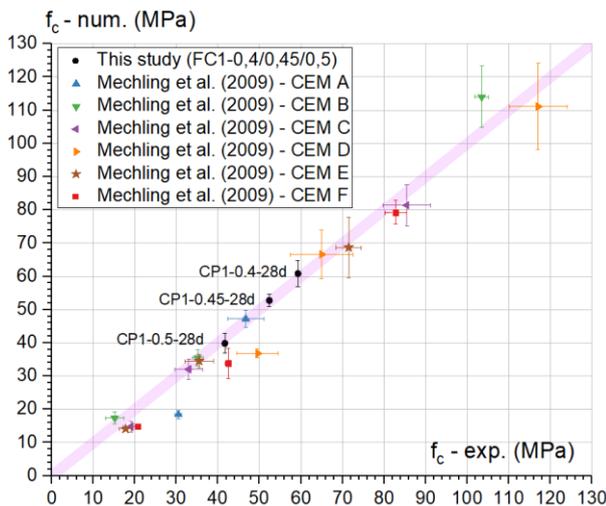
Table 2: Macroscopic properties of cement pastes: numerical values obtained by the simulation approach.

Cement paste	E (GPa)	f_t (MPa)	G_f (J/m²)
CP1-0.4-28d	17.6	7.54	7.9
CP1-0.4-14d	17.2	7.51	8.0
CP1-0.45-REF	16.0	6.77	6.7
CP1-0.45-14d	15.5	6.05	5.1
CP1-0.5-28d	14.4	5.25	5.3
CP1-0.5-14d	14.1	4.68	4.4
CP2-0.45-28d	14.8	5.45	4.7

Table 3: Macroscopic properties of cement pastes: experimental values obtained from inverse analysis.

Cement paste	E (GPa)	f_t (MPa)	G_f (J/m²)
CP1-0.4-28d	17.4	7.66	7.6
CP1-0.4-14d	17.7	7.50	7.4
CP1-0.45-REF	15.8	6.77	6.7
CP1-0.45-14d	15.3	6.62	5.4
CP1-0.5-28d	14.4	5.39	6.3
CP1-0.5-14d	14.6	5.29	6.1
CP2-0.45-28d	14.1	4.92	5.7

In the case of compression, Figure 7 shows the numerical and experimental estimations of the compressive strength of cement phases. The numerical values 60.8MPa, 52.7MPa and 39.8MPa for the w/c ratios of 0.4, 0.45 and 0.5 are very close to the experimental values of 59.3MPa, 52.4MPa and 41.7MPa. The small differences fall within the margin of error. As for the second series, the results show that for the most part, the micromechanical approach can estimate the compressive strength within a margin of ±2MPa. Certain examples deviate from this trend, where the strength is usually underestimated by up to 10MPa. This could be due to the overestimation of pore connectivity in cement pastes with high w/c ratios by the hydration model (see the next section for the limitations of the approach) which leads to the underestimation the strength. Another possible explanation is that the particle size distribution, which was only assumed for the cements A to F as no data was available, strongly affects the connectivity of the hydrates, leading to the underestimation of the strength. In any case, the numerical approach was able to quickly estimate the compressive strength without the need for calibration.

Figure 7: Compressive strength of cement pastes: comparison between experimental and numerical values (pink band = ±2MPa).

5 LIMITATIONS OF THE APPROACH

Despite its prediction of the macroscopic properties of well-hydrated cement pastes, some limitations are can be pointed out in the case of early-age testing. Following the same principles described above, the modelling approach correctly predicts of elastic moduli of early-age cement pastes (between 1 and 7 days), and fair estimation of the tensile strength (±1MPa) and fracture energy (±2J/m²) is given starting from the age of 7 days and for low w/c ratios (≤0.45). Beyond this, the macroscopic properties found by inverse analysis on experimental force-CMOD curves and the properties estimated numerically by the approach diverge for early age (1-2days) and high w/c ratios (>0.5). One possible explanation is that the hydration model underestimates the solid connectivity of the hydrates at early-age, leading to weaker bridges inside the matrix. Questions can also be raised concerning the macroscopic properties found from experimental tests on poorly hydrated cement pastes.

6 CONCLUSIONS AND PERSPECTIVES

The proposed micromechanical modelling approach has been used to simulate damage of cement paste at the microscale. The approach was first used to determine the effective phase properties needed for future simulations, then validated for a wide variety of cement mix designs. The modelling approach was able to predict the macroscopic properties of cement pastes and the localization of damage at the micro-level to a satisfactory degree.

The potential of this modelling approach can be extended further by exploiting the numerical results in multiscale modelling of concrete. In this case, the homogenised properties of cement paste can be injected in the cement matrix at the mesoscale (mortar or concrete). This way, the numerical modelling approach can be independent of experimental testing and does not require the recalibration of model parameters for each and every new mix design.

Furthermore, and since the cement phases

are explicitly represented inside the REV, distinct behaviour can be attributed to different phases. Thus, the micromechanical approach can be used to study the damage behaviour of cement paste in multiphysics simulations. Some potential uses of coupling the approach with internal viscoelastic or thermohygral mechanisms can be found in [22].

7 REFERENCES

[1] Constantinides, G. and Ulm, F. J., 2004. The effect of two types of C-S-H on the elasticity of cement-based materials: Results from nanoindentation and micromechanical modeling *Cement and Concrete Research* 34:67–80.

[2] Velez, K., Maximilien, S., Damidot, D., Fantozzi, G., and Sorrentino, F., 2001. Determination by nanoindentation of elastic modulus and hardness of pure constituents of Portland cement clinker *Cement and Concrete Research* 31:555–561.

[3] Němeček, J., Králík, V., Šmilauer, V., Polívka, L., and Jäger, A., 2016. Tensile strength of hydrated cement paste phases assessed by micro-bending tests and nanoindentation *Cement and Concrete Composites* 73:164–173.

[4] Dolado, J. S. and van Breugel, K., 2011. Recent advances in modeling for cementitious materials *Cement and Concrete Research* 41:711–726.

[5] Pellenq, R. J.-M. *et al.*, 2009. A realistic molecular model of cement hydrates. *Proceedings of the National Academy of Sciences of the United States of America* 106:16102–16107.

[6] Haecker, C.-J. *et al.*, 2005. Modeling the linear elastic properties of Portland cement paste *Cement and Concrete Research* 35:1948–1960.

[7] Ye, G., Sun, Z., Voigt, T., van Breugel, K., and Shah, S. P., 2004. A micromechanic model for characterization of cement paste at early age validated with experiments *International RILEM Symposium on Concrete Science and Engineering: A Tribute to Arnon Bentur*:1–11.

[8] Šmilauer, V. and Bittnar, Z., 2006. Microstructure-based micromechanical prediction of elastic properties in hydrating cement paste *Cement and Concrete Research* 36:1708–1718.

[9] Valentini, L. *et al.*, 2014. Simulation of the hydration kinetics and elastic moduli of cement mortars by microstructural modelling *Cement and Concrete Composites* 52:54–63.

[10] Bernard, F. and Kamali-Bernard, S., 2012. Predicting the evolution of mechanical and diffusivity properties of cement pastes and mortars for various hydration degrees – A numerical simulation investigation *Computational Materials Science* 61:106–115.

[11] Qian, Z., Schlangen, E., Ye, G., and Van Breugel, K., 2010. Prediction of mechanical properties of cement paste at microscale *Materiales de Construcción* 60:7–18.

[12] Luković, M., Schlangen, E., and Ye, G., 2015. Combined experimental and numerical study of fracture behaviour of cement paste at the microlevel *Cement and Concrete Research* 73:123–135.

[13] Hlobil, M., Šmilauer, V., and Chanvillard, G., 2016. Micromechanical multiscale fracture model for compressive strength of blended cement pastes *Cement and Concrete Research* 83:188–202.

[14] Bentz, D. P., 2000. CEMHYD3D: A Three-Dimensional Cement Hydration and Microstructure Development Modelling Package. Version 2.0 *NIST Interagency/Internal Report (NISTIR) - 6485*.

[15] Verpaux, P., Charras, T., and Millard, A., CASTEM 2000 une approche moderne du calcul des structures, *Calcul des structures et intelligences artificielle, Pluralis*, 1988. [Online]. Available: http://www-cast3m.cea.fr.

[16] Bullard, J. W. and Stutzman, P. E., 2006. Analysis of CCRL Portland Cement Proficiency Samples Number 151 and Number 152 Using the Virtual

Cement and Concrete Reference Laboratory *Cem. Concr. Res.* 36:1548–1555.

[17] Fichant, S., Pijaudier-Cabot, G., and La Borderie, C., 1997. Continuum damage modelling: Approximation of crack induced anisotropy *Mechanics Research Communications* 24:109–114.

[18] Fichant, S., La Borderie, C., and Pijaudier-Cabot, G., 1999. Isotropic and anisotropic descriptions of damage in concrete structures *Mechanics of Cohesive-frictional Materials* 4:339–359.

[19] Matallah, M., Farah, M., Grondin, F., Loukili, A., and Rozière, E., 2013. Size-independent fracture energy of concrete at very early ages by inverse analysis *Engineering Fracture Mechanics* 109:1–16.

[20] Bauchy, M., Laubie, H., Abdolhosseini Qomi, M. J., Hoover, C. G., Ulm, F.-J., and Pellenq, R. J.-M., 2015. Fracture toughness of calcium–silicate–hydrate from molecular dynamics simulations *Journal of Non-Crystalline Solids* 419:58–64.

[21] Radjy, F. and Hansen, T. C., 1973. Fracture of hardened cement paste and concrete *Cement and Concrete Research* 3:343–361.

[22] Rhardane, A., Élaboration d'une approche micromécanique pour modéliser l'endommagement des matériaux cimentaires sous fluage et cycles de gel-dégel, Ecole Centrale de Nantes, 2018.

[23] Šmilauer, V., CemBase - cement database for Nanocem. [Online]. Available: http://mech.fsv.cvut.cz/~smilauer/index. php?id=cembase.

[24] Mechling, J.-M., Lecomte, A., and Diliberto, C., 2009. Relation between cement composition and compressive strength of pure pastes *Cement and Concrete Composites* 31:255–262.